



Treatment of oily wastewater by combining ozonation and microfiltration

Zsolt László Kiss, Lajos Kocsis, Gábor Keszthelyi-Szabó, Cecilia Hodúr,
Zsuzsanna László*

*Faculty of Engineering, University of Szeged, Moszkvai krt. 9, H-6725 Szeged, Hungary, Tel. +0036 62 546561;
email: zsizsu@mk.u-szeged.hu*

Received 11 April 2014; Accepted 16 June 2014

ABSTRACT

In process industries, a large amount of wastewater is generated in the form of oil-in-water emulsions, which cannot be treated effectively using traditional physical methods. The aim of our investigation was to examine the applicability of the membrane technique and the effect of pre-ozonation in oily wastewater treatment. Pre-ozonation followed by microfiltration (MF) was investigated to determine the main effects of ozonation on the oily water and the filtration parameters such as permeate flux, organic content retention and membrane fouling. Experiments were carried out with a laboratory-scale batch-stirred filtration device, using polyethersulphone MF membranes with a pore size 0.2 μm . The model oily wastewater that was used in these experiments contained petroleum. The results demonstrated that the chemical oxygen demand could be eliminated more effectively through the combination of ozone pre-treatment and membrane filtration, compared to membrane filtration alone.

Keywords: Microfiltration; Ozone treatment; Oily wastewater; Membrane fouling

1. Introduction

Oily wastewater emulsions discharged by process industries are prominent amongst the major pollutants of the aquatic environment. A large amount of oil-contaminated water is generated worldwide on a daily basis [1]. Several industries, such as steel, metallurgical, petrochemical, transportation, textile and petroleum industries, produce oily wastewater emulsions in the concentration range of 50–1,000 mg L^{-1} [2]. The separation of oil from a dilute emulsion of oil and water is a problem that occurs in a number of aqueous discharges [3].

Conventional methods of oily wastewater treatment include gravity separation, air flotation, coagulation, demulsification and biochemical treatment, all of which have intrinsic disadvantages such as low efficiencies, high operation costs and recontamination problems. These conventional technologies are not efficient enough to treat stable oil-in-water emulsions that contain oil droplets smaller than 20 μm , especially when the oil concentration is reasonably low and the droplets are finely dispersed. To overcome this problem and to achieve the minimum threshold limits for releasing treated wastewater into the discharge (or drain), membrane processes are increasingly being investigated for the treatment of oil-in-water

*Corresponding author.

*Presented at the Conference on Desalination for the Environment: Clean Water and Energy
11–15 May 2014, Limassol, Cyprus*

emulsions [4], and there are many articles related to threshold limits and ultrafiltration (UF)/microfiltration (MF) of oily wastewaters. Nowadays, membrane separation techniques are continuously receiving increasing attention for the treatment of water containing high levels of organic matter, owing to their remarkable advantages such as superior water quality, the removal of a wide range of contaminants, easier control of the operation parameters and space saving capabilities. However, the decline of membrane permeate flux during operation, due to fouling, is a significant limiting factor in the development and applicability of these membrane separation processes [5,6].

MF of oil-in-water emulsions has been investigated experimentally in recent decades. This membrane process has shown to be effective and represents a possible separation solution [7–11]. Membrane materials are also important for oil-in-water emulsion separation, and it has been recognised that hydrophilic materials are less sensitive to adsorption compared with hydrophobic ones; therefore, hydrophilic membrane materials may be considered as a key solution in reducing membrane fouling [12]. Pre-oxidation results in improved flocculation efficiency and particle removal during filtration [13]. In ozone-UF systems, the ozone treatment, like a pre-treatment, always causes a remarkable decrease in the cake resistance (R_c) and an increase in the fouling resistance (R_f) [14]. Based on measurements of the particle-size distribution and the zeta potential, a reduction in R_c through ozonation was attributed to the increasing particle size, which was caused by “ozone-induced particle destabilisation” [14].

This article addresses the MF of oil-in-water emulsions when using different pre-ozonation times before the filtration experiment. MF studies were targeted to study the effect of pre-ozonation on the oily water emulsion and the filtration parameters (i.e. flux, filtration resistances and oil rejection). Using experimental flux decline data, fouling mechanisms during MF were analysed and modelled.

2. Materials and methods

2.1. Materials

A model oil-in-water emulsion, with an oil concentration of 0.01 wt.%, was prepared from petroleum (produced by N6grádi Erd6k6mia Kft. Hungary) using ultrasonication for 20 min.

2.2. Experimental design

The experimental set-up is shown in Fig. 1. The oil-in-water emulsion was treated with ozone for a

given time and the treated solution was then promptly used as the feed in the MF experiments.

Ozone was produced from oxygen (Linde, 3.5) using a flow-type ozone generator (BMT 802X, Germany). The ozone-containing gas was bubbled continuously through a batch reactor during the treatment. The volume of treated water was 0.5 L and the gas flow rate was 1 L min⁻¹. The ozone concentration in the gas was measured before and after the reactor using a UV spectrophotometer (WPA Lightwave S2000) at a wavelength of 254 nm. The amount of absorbed ozone was 1.4, 4.7, 12.84, 19.07, 27.42, 51.46 and 89.07 mg L⁻¹ at treatment times of 2, 4, 6, 8, 10, 12 and 14 min, respectively. The membrane filtration experiments were carried out in a batch-stirred cell (Millipore, XFUF04701) with a capacity of 50 cm³. Flat-sheet polyethersulphone (PES) membranes with a pore size of 0.2 μm and a membrane effective area of 0.001734 m² were used (PL series, Millipore). Before each MF experiment, the membrane was immersed in distilled water overnight. The initial feed volume was 50 cm³ and experiments were carried out at 10 kPa until 10 cm³ of the total sample had been filtered at a stirring speed of 50 rpm. Determination of the chemical oxygen demand (COD) was based on the standard method, which involves potassium dichromate oxidation. For the analyses, standard test tubes (Lovibond) were used. The digestions were carried out in a COD digester (Lovibond, ET 108) and the COD values were measured with a COD photometer (Lovibond PC-CheckIt). The particle-size distribution (within the range 0.1–1,000 μm) was measured using a Mastersizer 2000 (Malvern Instruments); the injection temperature was 20°C. Viscosity measurements were carried out with a Vibro viscometer (AND SV-10 A&D Company, Japan) in a temperature-controlled water bath (Cole Palmer, USA) at a constant temperature of 20.0 ± 0.1°C. The density of each solution was measured at 20°C with a Density 30PX digital density meter (Mettler Toledo, Japan).

Diffusion coefficients were determined at 20°C using an Armfield CERb apparatus (Armfield, Great Britain), according to the manufacturer’s instructions. Measurements were carried out with a 0.01% petroleum emulsion by measuring the change in conductivity in distilled water. The diffusion coefficient of petroleum was 3.64 × 10⁻⁹ m² s⁻¹ whereas after ozonation for 12 min, it was 4.65 × 10⁻⁹ m² s⁻¹.

Membrane hydrophobicity was quantified by measuring the contact angle that was formed between the membrane surface (before and after filtration of solutions) and water. Contact angles were measured using the sessile drop method (Dataphysics Contact Angle System OCA15Pro, Germany).

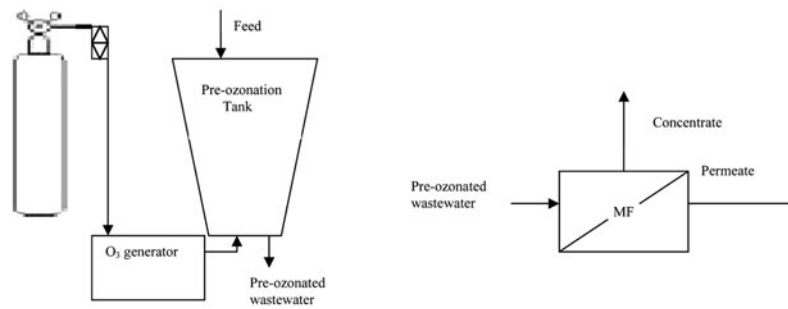


Fig. 1. Experimental design of the pre-ozonation (left) and MF (right) processes.

2.3. Fouling models

2.3.1. Filtration laws

Fouling mechanisms that have been widely used include cake filtration, intermediate filtration, standard pore blocking and complete pore blocking; [7,15–17] the filtration laws are given in Table 1.

In Eqs. (1)–(8), J is the flux, J_0 is the initial flux, the various k values represent the fouling coefficients, K_c is the solute mass transfer coefficient (m s^{-1}) and A is a constant. In Eq. (8), A can be expressed as:

$$A = \sqrt{\frac{k_c}{2K_c}} \quad (9)$$

The K_c value was calculated from the following correlations: [18,19]

$$K_c = 0.285 \frac{D}{b} \cdot \text{Re}^{0.55} \cdot \text{Sc}^{0.33} \quad \text{if } \text{Re} < 3,200 \quad (10)$$

$$K_c = 0.0443 \frac{D}{b} \cdot \text{Re}^{0.75} \cdot \text{Sc}^{0.33} \quad \text{if } \text{Re} > 3,200 \quad (11)$$

where $\text{Re} = \frac{\omega b^2 \rho}{\eta}$, $\text{Sc} = \frac{\eta}{\rho D}$, b is the stirring radius, ω is the stirring velocity (in rad s^{-1}), D is the diffusion coefficient (in $\text{m}^2 \text{s}^{-1}$), η is the dynamic viscosity (Pas) and ρ is the density (kg m^{-3}).

By assuming a convection–diffusion mechanism during the filtration process, the flux is generally expressed by a simplified Equation: [20]

$$J = K_c \cdot \ln \left(\frac{c_M - c_P}{c_F - c_P} \right) \quad (12)$$

where c_M is the concentration on the membrane surface, c_P is the permeate concentration and c_F is the feed concentration. The polarisation layer concentration was calculated according to the following Equation:

$$c_M = (c_F - c_P) e^{J_c} + c_P \quad (13)$$

where J_c is the constant flux at the end of the concentration test.

2.3.2. Resistance-in-series model

The membrane resistance (R_M) was calculated as: [21]

$$R_M = \frac{\Delta p}{J_w \eta_w} \quad (\text{m}^{-1}) \quad (14)$$

where Δp is the pressure difference between the two sides of the membrane (Pa), J_w is the water flux of the clean membrane and η_w is the viscosity of the water (Pas).

The R_F was determined by measuring the water flux through the membrane after the MF and rinsing it with deionised water to remove any particles of the residue layer from the surface, and then by subtracting the resistance of the clean membrane:

$$R_F = \frac{\Delta p}{J_{WA} \eta_w} - R_M \quad (15)$$

where J_{WA} is the water flux after the concentration test. The resistance of the polarisation layer (R_P) can be calculated as:

$$R_P = \frac{\Delta p}{J_C \eta_{ww}} - R_F - R_M \quad (16)$$

R_T , the total resistance (m^{-1}), can be evaluated from the steady-state flux by using the resistance-in-series model:

$$R_T = R_M + R_F + R_P \quad (17)$$

Table 1
Filtration laws

| Fouling mechanism | Filtration law | Constant pressure filtration (J_0 A = constant) |
|--|--|--|
| Complete pore blocking | $J = J_0 e^{-k_b t}$ | (1) $\ln J = \ln J_0 - k_b \cdot t$ (5) |
| Gradual pore blocking (standard pore blocking) | $J = J_0 (1 + \frac{1}{2} K_s (A \cdot J_0)^{0.5} \cdot t)^{-2}$ | (2) $\frac{1}{\sqrt{J}} = \frac{1}{\sqrt{J_0}} + k_s \cdot t$ $k_s = 0.5 k_s A^{0.5}$ (6) |
| Intermediate filtration | $J = J_0 \cdot (1 + K_i \cdot A \cdot J_0 \cdot t)^{-1}$ | (3) $\frac{1}{J} = \frac{1}{J_0} + k_i \cdot t$ $k_i = K_i A$ (7) |
| Cake filtration | $J = J_0 (1 + 2K_c (A \cdot J_0)^2 \cdot t)^{-0.5}$ | (4) $\frac{1}{J^2} = \frac{1}{J_0^2} + k_c \cdot t$ $k_c = 2K_c A^2$ (8) |

And the volume reduction ratio (VRR) can be determined using the following Equation:

$$\text{VRR} = \frac{V_{\text{feed}}}{V_{\text{feed}} - V_{\text{perm}}} \quad (18)$$

where V_{feed} is the feed volume (cm^3) and V_{perm} is the permeate volume (cm^3).

The selectivity of a membrane for a given solute can be expressed by the average retention (R): [22]

$$R = \left(1 - \frac{c}{c_0}\right) \cdot 100\% \quad (19)$$

where c is the average concentration of the solute in the permeate phase and c_0 is the concentration of the solute in the feed.

3. Results and discussion

3.1. Effect of pre-ozonation

In the first series of experiments, the effect of ozone treatment on the concentration of organic (oxidisable) compounds was investigated. Fig. 2(a) demonstrates that petroleum hydrocarbon compounds result in a high COD value, and that they can be reduced in the wastewater. The turbidity also

decreased after ozonation; the petroleum hydrocarbon component is decomposed, resulting in a lower turbidity value.

The conductivity increased with the duration of ozonation, which can be explained by the production of small organic acids originating from the degradation of hydrocarbons (Fig. 2(b)). This phenomenon is consistent with the changes in pH, which is decreased because of the presence of the organic acids formed by the oxidation of hydrocarbons.

In the next series of experiments, the effect of pre-ozonation on the emulsified particle size was examined. It was found that a longer ozonation time (12 min) resulted in a larger emulsified particle size (Fig. 3). The emulsified particle size was originally $0.55 \mu\text{m}$ in the 0.01% petroleum emulsion, $0.56 \mu\text{m}$ after ozone treatment for 8 min and $0.59 \mu\text{m}$ after ozone treatment for 12 min. This phenomenon can be attributed to the effect of ozone; the ozone molecules react with long-chain hydrocarbons producing micelle-forming amphiphilic molecules, which can stabilise the droplets by forming a “bridge” between the surface of the oil droplet and the water.

3.2. Effect of pre-ozonation on MF

In the next series of experiments, the pre-ozonated oil emulsions were filtered through $0.2 \mu\text{m}$ PES membranes. Fig. 4(a) depicts stabilised fluxes as a function

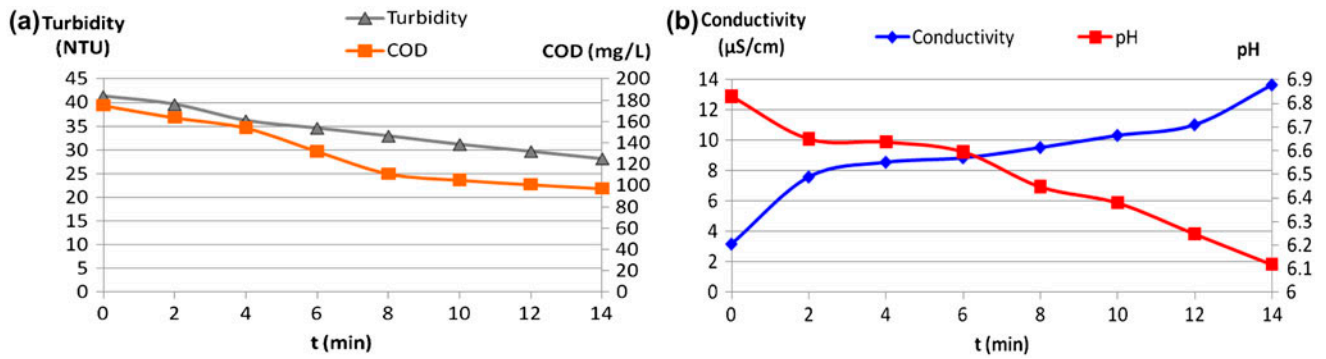


Fig. 2. (a) Effect of ozone treatment on COD and turbidity of wastewater and (b) the changes of conductivity and pH during ozone treatment.

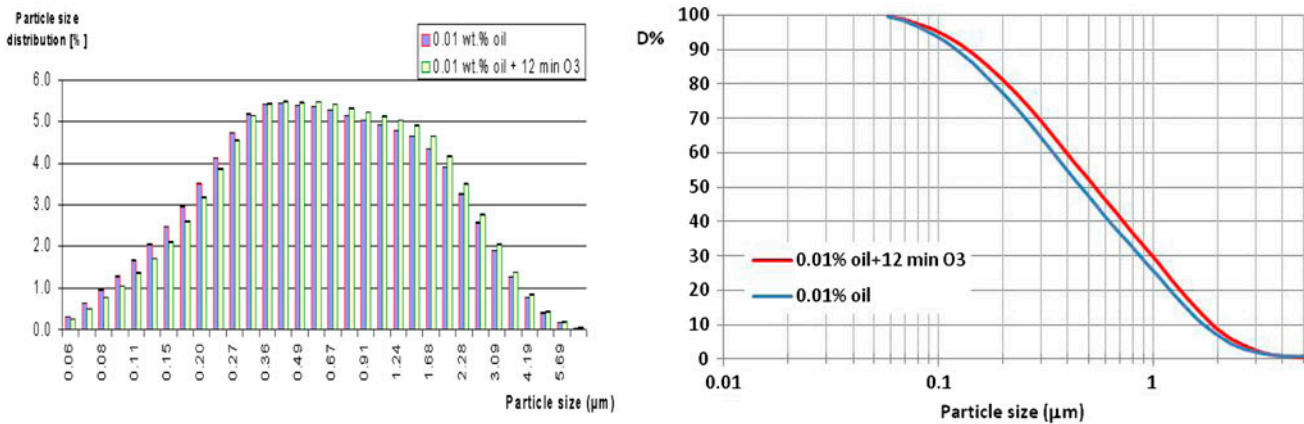


Fig. 3. Particle-size distribution of oily wastewater after 12 min ozonation (left) and without ozonation (right) at 20°C.

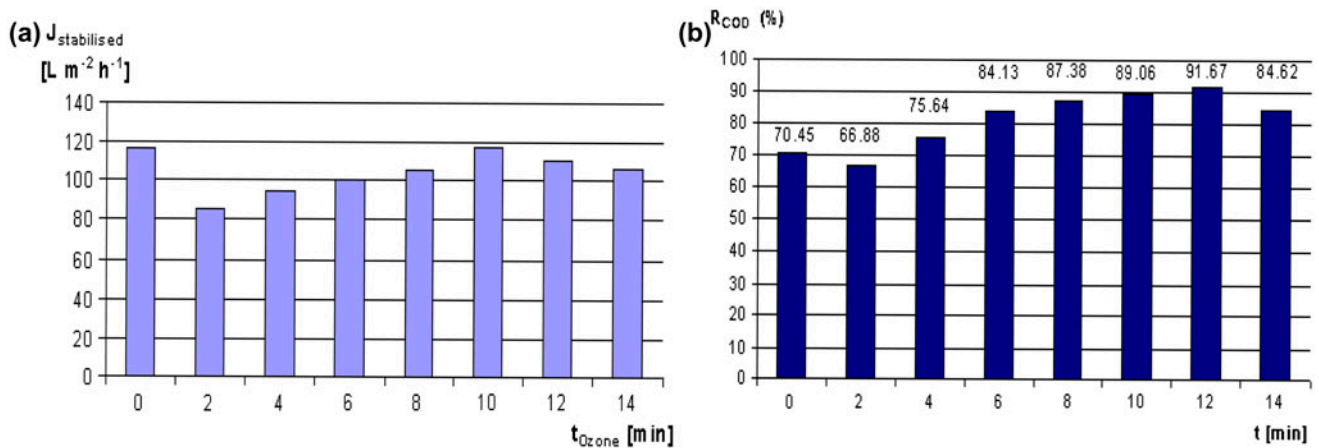


Fig. 4. (a) Stabilised fluxes as a function of the ozonation time and (b) COD retention as a function of ozonation time.

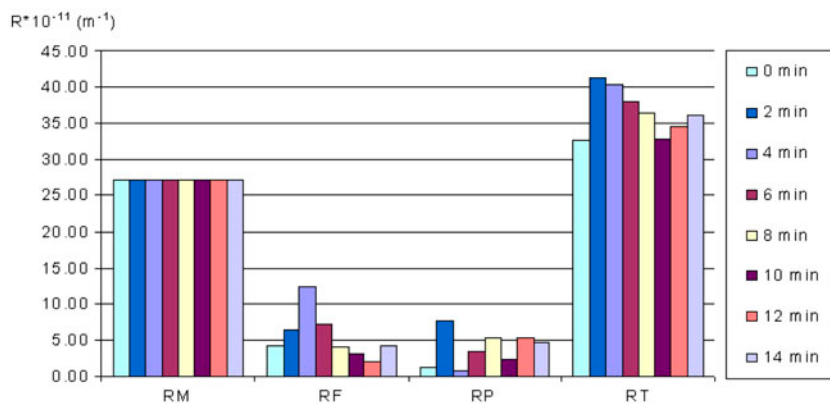


Fig. 5. Filtration resistances.

of ozone treatment time. It was found that pre-ozonation decreased the flux, but increasing the ozonation time increased the stabilised flux. The COD retention changed with flux; lower ozone doses decreased the COD retention, whereas further ozonation increased the COD retention. This can be explained by ozone-induced decomposition of hydrocarbon molecules. The smaller reaction products were able to pass through the membrane, resulting in a lower COD in the retention phase (Fig. 4(b)). However, in oil emulsions in cross-flow MF above the membrane surface, the droplets may become deformed, break up and penetrate into the pores [10], as the size of the drop is bigger than the size of the pore [11]. Further ozone treatment may cause micelle formation of molecules (Fig. 3), resulting in more particles that are less deformable and, therefore, achieving a higher COD retention. The highest COD retention value was achieved after ozone treatment for 12 min.

Calculation of the filtration resistances also showed that the ozone treatment affected both the fouling and polarisation layer resistances. Shorter ozonation times resulted in higher R_F values (Fig. 5), explaining the lower flux. Further ozonation decreased the pore fouling and the parallel polarisation layer resistances increased in accordance with the micelle formation effect of ozone treatment. The COD retention value (Fig. 4(b)) and filtration resistances indicate that the optimum time for pre-ozonation before membrane separation is 12 min.

As the ozone treatment changes the chemical nature of the particles in the emulsion (e.g., the polarity of large molecules), the interaction between the solution and the membrane surface can also change. The contact angle measurements showed that after filtering the oily water, the membrane surface became less hydrophilic than the clean membrane surface (the contact angle

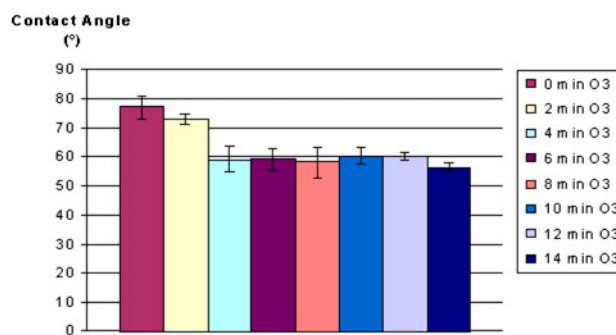


Fig. 6. Changes of contact angle as a function of ozonation time.

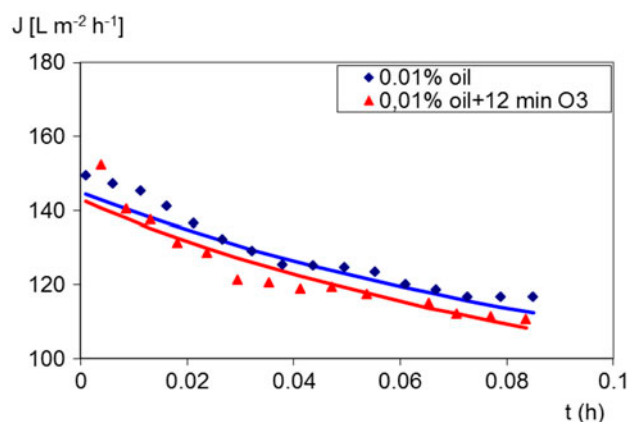


Fig. 7. Permeate fluxes as a function of the filtration time for untreated and 12 min ozone-treated solutions. The continuous lines show the fitted data, which were calculated using Eq. (4).

increased to $77.06 \pm 4.16^\circ$ from $59.42 \pm 3.00^\circ$), but the filtration of ozone-treated solutions decreased the hydrophobicity of the membrane with increasing ozonation times (Fig. 6). This phenomenon explains the

Table 2
Results of the calculations

| Experiment | k_c ($\text{m}^4 \text{L}^{-6} \text{h}^{-1}$) | J_0 ($\text{L m}^{-2} \text{h}^{-1}$) | A (-) | K_c (m s^{-1}) | c_M (wt.%) | c_P (wt.%) |
|--------------------------|--|---|---------|-----------------------------|--------------|--------------|
| MF | 1,267,200 | 147.12 | 172,400 | 2.24×10^{-05} | 0.051 | 0.00296 |
| 12 min O_3 + MF | 1,710,000 | 148.48 | | 2.64×10^{-05} | 0.046 | 0.00083 |

increasing flux with increasing ozonation time; the increased hydrophilic character of the membrane helps to pass water through the membrane.

3.3. Filtration model

In order to obtain a more sophisticated description of the ozone treatment effects, the filtration models were fitted to flux-time functions of the 0.01% oily water as well as the solution that had been subjected to ozonation for 12 min. The fouling coefficient, initial flux, mass transfer coefficient and concentration of oil on the surface of the membrane were calculated and compared. Filtration models were fitted to the experimental data, analysis of which showed that the cake filtration model (Eq. (4)) provides the best correlation ($R^2 = 0.96$ and 0.91 for the two samples, respectively). By fitting Eq. (8) to experimental data, the initial flux value, J_0 , and the k_c fouling coefficient could be determined for each sample. Assuming a convection–diffusion mechanism occurred during filtration, the mass transfer coefficients and the oil concentration on the membrane surface could be calculated using Eqs. (12) and (13). The results of the calculations are summarised in Table 2.

The results show that the k_c fouling coefficient increased with prolonged ozone treatment (in accordance with the filtration resistances), whereas the initial fluxes did not change significantly. The mass transfer coefficient was higher in ozone-treated solutions, owing to a higher diffusion coefficient. Although the polarisation layer resistance was higher in the ozone-treated solution, the concentration on the surface of the membrane (c_M) was lower. This can be explained using the concentration polarisation model; concentration gradients between the bulk-feed solution and the membrane surface can cause additional diffusion fluxes, which are expressed more in the ozone-treated solution because the higher diffusion coefficient of the particles contributes to a decrease in the flux of the membrane (Fig. 7).

4. Conclusions

Untreated and ozone-treated petroleum (0.01 wt.%) oil-in-water emulsions were filtered with a 0.2- μm PES

MF membrane. It was found that pre-ozonation changed the chemical nature of the emulsified particles, causing a change in the interactions that occurred between the solution and the membrane surface, which thus affected the filtration parameters. A short ozone treatment time caused degradation of long-chain hydrocarbon molecules, which were formed when smaller molecules foul the membrane, resulting in a decreased permeate flux and decreased COD retention. Further ozone treatment led to a considerable amount of large amphiphilic molecules to be produced; micelle formation could occur, resulting in an increased particle size and fewer deformable particles. These particles cannot foul the membrane pores, but they are (i) accumulated on the surface of the membrane and (ii) diffused back into the bulk feed solution, causing an increased polarisation resistance and increased COD retention.

Acknowledgements

The authors are grateful for the financial support provided by the OTKA project (project number OTKA K105021). This research was realised within the framework of the TÁMOP 4.2.4 A/2-11-1-2012-0001 National Excellence Program—Elaborating and Operating an Inland Student and Researcher Personal Support System Convergence Program. The project was also subsidised by the European Union and co-financed by the European Social Fund.

List of symbols

| | |
|----------|--|
| J | — flux ($\text{L m}^{-2} \text{h}^{-1}$) |
| J_0 | — initial flux |
| J_c | — constant flux at the end of the concentration test ($\text{L m}^{-2} \text{h}^{-1}$) |
| J_{WA} | — water flux after concentration tests ($\text{L m}^{-2} \text{h}^{-1}$) |
| J_w | — water flux ($\text{L m}^{-2} \text{h}^{-1}$) |
| k_c | — fouling coefficient |
| A | — experimental constant |
| K_c | — mass transfer coefficient (m s^{-1}) |
| B | — stirring radius (m) |
| Ω | — stirring velocity (rad s^{-1}) |
| D | — diffusion coefficient ($\text{m}^2 \text{s}^{-1}$) |
| Re | — Reynolds number |
| Sc | — Schmidt number |
| η | — dynamic viscosity (Pas) |

| | |
|-------------|--|
| ρ | — density (kg m ⁻³) |
| c_M | — concentration on membrane surface (wt.%) |
| c_P | — permeate concentration (wt.%) |
| c_F | — feed concentration (wt.%) |
| R_M | — membrane resistance (m ⁻¹) |
| R_F | — fouling resistance (m ⁻¹) |
| R_P | — polarisation layer resistance (m ⁻¹) |
| R_T | — total resistance (m ⁻¹) |
| Δp | — transmembrane pressure (Pa) |
| η_w | — viscosity of the water (Pas) |
| η_{ww} | — viscosity of the wastewater (Pas) |
| VRR | — volume reduction ratio (-) |
| R | — retention (%) |

References

- [1] J. Cakl, I. Bauer, P. Doleček, P. Mikulášek, Effects of backflushing conditions on permeate flux in membrane crossflow microfiltration of oil emulsion, *Desalination* 127 (2000) 189–198.
- [2] D. Vasanth, G. Pugazhenth, R. Uppaluri, Cross-flow microfiltration of oil-in-water emulsions using low cost ceramic membranes, *Desalination* 320 (2013) 86–95.
- [3] I.W. Cumming, R.G. Holdich, I.D. Smith, The Rejection of oil by microfiltration of a stabilised kerosene/water emulsion, *J. Membr. Sci.* 169 (2000) 147–155.
- [4] M. Zare, F.Z. Ashtiani, A. Fouladitajar, CFD modeling and simulation of concentration polarization in microfiltration of oil-water emulsions; Application of an Eulerian multiphase model, *Desalination* 324 (2013) 37–47.
- [5] Y. Yang, R. Chen, W. Xing, Integration of ceramic membrane microfiltration with powdered activated carbon for advanced treatment of oil-in-water emulsion, *Sep. Purif. Technol.* 76 (2011) 373–377.
- [6] H. Zhou, D.W. Smith, Advanced technologies in water and wastewater treatment, *J. Environ. Eng. Sci.* 1 (2002) 247–264.
- [7] A. Fouladitajar, F.Z. Zokae Ashtiani, A. Okhovat, B. Dabir, Membrane fouling in microfiltration of oil-in-water emulsions: A comparison between constant pressure blocking laws and genetic programming (GP) model, *Desalination* 329 (2013) 41–49.
- [8] E. Iritani, S. Matsumoto, N. Katagiri, Formation and consolidation of filter cake in microfiltration of emulsion-slurry, *J. Membr. Sci.* 318 (2008) 56–64.
- [9] A. Ullah, R.G. Holdich, M. Naem, V.M. Starov, Shear enhanced microfiltration and rejection of crude oil drops through a slotted pore membrane including migration velocities. *J. Membr. Sci.* 421–422 (2012) 69–74.
- [10] T. Darvishzadeh, N.V. Priezjev, Effects of crossflow velocity and transmembrane pressure on microfiltration of oil-in-water emulsions, *J. Membr. Sci.* 423–424 (2012) 468–476.
- [11] A. Ullah, R.G. Holdich, M. Naem, V.M. Starov, Stability and deformation of oil droplets during microfiltration on a slotted pore membrane, *J. Membr. Sci.* 401–402 (2012) 118–124.
- [12] L. Li, L. Ding, Z. Tu, Y. Wan, D. Clause, J. Lanoisellé, Recovery of linseed oil dispersed within an oil-in-water emulsion using hydrophilic membrane by rotating disk filtration system, *J. Membr. Sci.* 342 (2009) 70–79.
- [13] R.D. Paode, M. Chandrakanth, G.L. Amy, J.T. Gramith, D.W. Ferguson, Ozone versus ozone/peroxide induced particle destabilization and aggregation: A pilot study, *Ozone Sci. Eng.* 17 (2005) 25–51.
- [14] H. Hyung, S. Lee, J. Yoon, C.-H. Lee, Effect of preozonation of flux and water quality in ozonation-ultrafiltration hybrid system for water treatment, *Ozone Sci. Eng.* 22 (2000) 637–652.
- [15] B. Hu, K. Scott, Microfiltration of water in oil emulsions and evaluation of fouling mechanism, *Chem. Eng. J.* 136 (2008) 210–220.
- [16] S. Banerjee, S. De, An analytical solution of sherwood number in a stirred continuous cell during steady state ultrafiltration, *J. Membr. Sci.* 389 (2012) 188–196.
- [17] Zs. L. Kiss, Sz. Kertész, S. Beszédes, C. Hodúr, Z. László, Investigation of parameters affecting the ultrafiltration of oil-in-water emulsion wastewater, *Desalin. Water Treat.* (2013) 1–7, doi: [10.1080/19443994.2013.795323](https://doi.org/10.1080/19443994.2013.795323).
- [18] S.R. Jadhav, N. Verma, A. Sharma, P.K. Bhattacharya, Flux and retention analysis during micellar enhanced ultrafiltration for the removal of phenol and aniline, *Sep. Purif. Technol.* 24 (2001) 541–557.
- [19] S. Nicolas, B. Balannec, F. Beline, B. Bariou, Ultrafiltration and reverse osmosis of small non-charged molecules: A comparison study of rejection in a stirred and an unstirred batch cell, *J. Membr. Sci.* 164 (2000) 141–155.
- [20] M. Schwarze, D.K. Le, S. Wille, A. Drews, W. Arlt, Stirred cell ultrafiltration of aqueous micellar TX-100 solutions. *Sep. Purif. Technol.* 74 (2010) 21–27.
- [21] Sz. Kertesz, Zs. Laszlo, E. Forgacs, G. Szabo, C. Hodur, Dairy wastewater purification by vibratory shear enhanced processing, *Desalin. Water Treat.* 37 (2012) 1–7.
- [22] Y. Pan, W. Wang, T. Wang, P. Yao, Fabrication of carbon membrane and microfiltration of oil-in-water emulsion: An investigation on fouling mechanisms, *Sep. Purif. Technol.* 57 (2007) 388–393.